

European Geosciences Union General Assembly 2015, EGU

Division Energy, Resources & Environment, ERE

## Sensitivity of a 3D geothermal model of Berlin with respect to upper boundary conditions

Maximilian Frick<sup>a,b,\*</sup>, Magdalena Scheck-Wenderoth<sup>a,c</sup>, Judith Sippel<sup>a</sup>, Mauro Cacace<sup>a</sup>

<sup>a</sup>Section 4.4 Basin Analysis, GFZ German Research Centre for Geosciences, Telegrafenberg, 14473 Potsdam, Germany

<sup>b</sup>University Potsdam, Institute for Earth and Environmental Science, Karl-Liebknecht-Str.24, 14476 Potsdam, Germany

<sup>c</sup>RWTH Aachen, School of Geosciences, Templergraben 55, 52056 Aachen, Germany

---

### Abstract

The goal of this study is to quantify the influences of upper hydraulic and temperature boundary conditions on temperatures as calculated by 3D numerical simulations of coupled fluid-and-heat transport for the subsurface of Berlin. Both, the underlying structural model, as well as the sensitivity analysis are data-driven. The results show that the subsurface thermal field is strongly influenced by hydraulic and thermal boundary conditions. Findings of this study suggest that in the model area conductive heat transport processes are able to compensate the influence of advection by pressure gradients. Also, anthropogenic influences on the subsurface thermal field could be quantified.

© 2015 The Authors. Published by Elsevier Ltd. This is an open access article under the CC BY-NC-ND license

(<http://creativecommons.org/licenses/by-nc-nd/4.0/>).

Peer-review under responsibility of the GFZ German Research Centre for Geosciences

**Keywords:** 3D geological model; Coupled fluid and heat transport; Sensitivity analysis; Boundary conditions

---

### 1. Introduction

The present-day temperature configuration in sedimentary basins is influenced by different coupled physical processes comprising principally diffusion of heat by conduction and advective forces by groundwater circulating within the pore space of permeable sedimentary rocks. Several driving mechanisms of regional groundwater flow can

---

\* Corresponding author. Tel.: +49-331-288-2828.

E-mail address: [mfrick@gfz-potsdam.de](mailto:mfrick@gfz-potsdam.de)

be distinguished within sedimentary basins, e.g. gravitational or topography-driven flow, overpressure flow, or flow due to buoyant forces within the fluid. The relative role that each of these processes play in affecting the present-day thermal configuration of a basin depends principally on the local hydrogeological setting and on the external (e.g. climatic and anthropogenic) surface forcing. Despite a relative flat topography and the absence of recent tectonic activity, within the North German Basin latest 3D numerical investigations of coupled fluid and heat transport have provided strong evidence for the presence of a regional hydro-thermal regime influenced by conduction of heat from the deeper crust overprinted within the shallower sedimentary units by a regional component of pressure (topographically) driven groundwater flow. While able to account for the first order aspect of the present-day thermal configuration, comparison of predicted and observed temperatures showed a local and systematic misfit. This misfit occurs predominantly at shallower depth levels (first couple of kilometers), with model results being generally colder than measurements. Based on systematic analysis of these results, two major causes for the observed discrepancy between model and observations have been hypothesized; (1) a lack in details of the implemented representation of the surface hydraulic and thermal conditions, and (2) an oversimplified structural diversification of the most shallow Quaternary and Tertiary aquifer complexes.

This study is part of ongoing activities aiming at investigating and quantifying the relevance of the aforementioned aspects focusing on the present-day thermal configuration beneath the city of Berlin, capital city of Germany. The objective is to carry out a systematic analysis of the influence of different hydraulic and thermal surface configurations and quantify their relative contribution to the present-day thermal configuration of the study area with a special focus on its geothermal potential. At this purpose an existing geological model of the subsurface of Berlin [1] is adopted to carry out numerical thermal and hydraulic coupled simulations (see section 2, 3). Different boundary conditions are imposed to represent different scenarios in terms of surface temperature and groundwater dynamics (see section 4). Direct comparison between the different model outcomes is then carried out in order to quantify the effects of the shallow configuration on the regional hydraulic and thermal setting. Therefore, the merit of this study is twofold. On the one hand with its direct application to the city of Berlin, it provides useful insights in understanding the present-day regional thermal configuration in terms of the major physical driving processes. On the other hand, the study outlines an approach that could be of assistance to quantify uncertainties often encountered in coupled hydraulic and thermal simulations in complex basin settings.

## 2. Geological Setting of the Structural Model

In order to carry out our sensitivity study we used an existing 3D structural model of Berlin based on published data [2-4] and newly integrated borehole-derived formation-top data [1]. This model differentiated 16 units for the sedimentary basin fill (Fig. 1a) and 5 units for the underlying basement, namely Permian Volcanics, Permian, Upper Crust, Lower Crust and Lithospheric Mantle. In our study we limit the vertical extension of the input model to comprise the major sedimentary sequences. Therefore, we cut the lithosphere-scale model at a constant depth of -6000 m.a.s.l., thus integrating all 16 sedimentary units overlying the volcanics. The sedimentary succession is of Permian to Cenozoic age and consists predominantly of clastics, carbonates and rock salt. The latter is present in form of the Permian Zechstein salt which highly controlled and modified the geometry of the post salt succession. The Zechstein salt has been mobilized from Mid Triassic times onward [5], has locally increased thicknesses of more than 3400 m and shows a complex topological configuration (Fig. 1b). Mesozoic sediments are mainly composed of consolidated clastics or carbonates. Of special interest for geothermal applications are the Middle Triassic (Middle Buntsandstein) and Permian Sedimentary Rotliegend. Both units consists of sandstones consolidated to varying degrees and have a porosity and permeability high enough to be considered as potential target horizons for geothermal installations beneath Berlin [6]. The younger Cenozoic sediments are mainly composed of unconsolidated clastics. They contain the main shallow aquifer system providing the city of Berlin with fresh water. In this respect the Tertiary Rupelian Clay unit plays an important role as an interbedded aquitard separating the shallow freshwater aquifers from the deeper saline aquifers [7]. This aquitard is, however, discontinuous in the Berlin area (due to non-deposition, erosional unconformities and erosional subglacial channels) thus local hydrodynamic connections may exist between the two aquifers at depth (Fig. 1c).

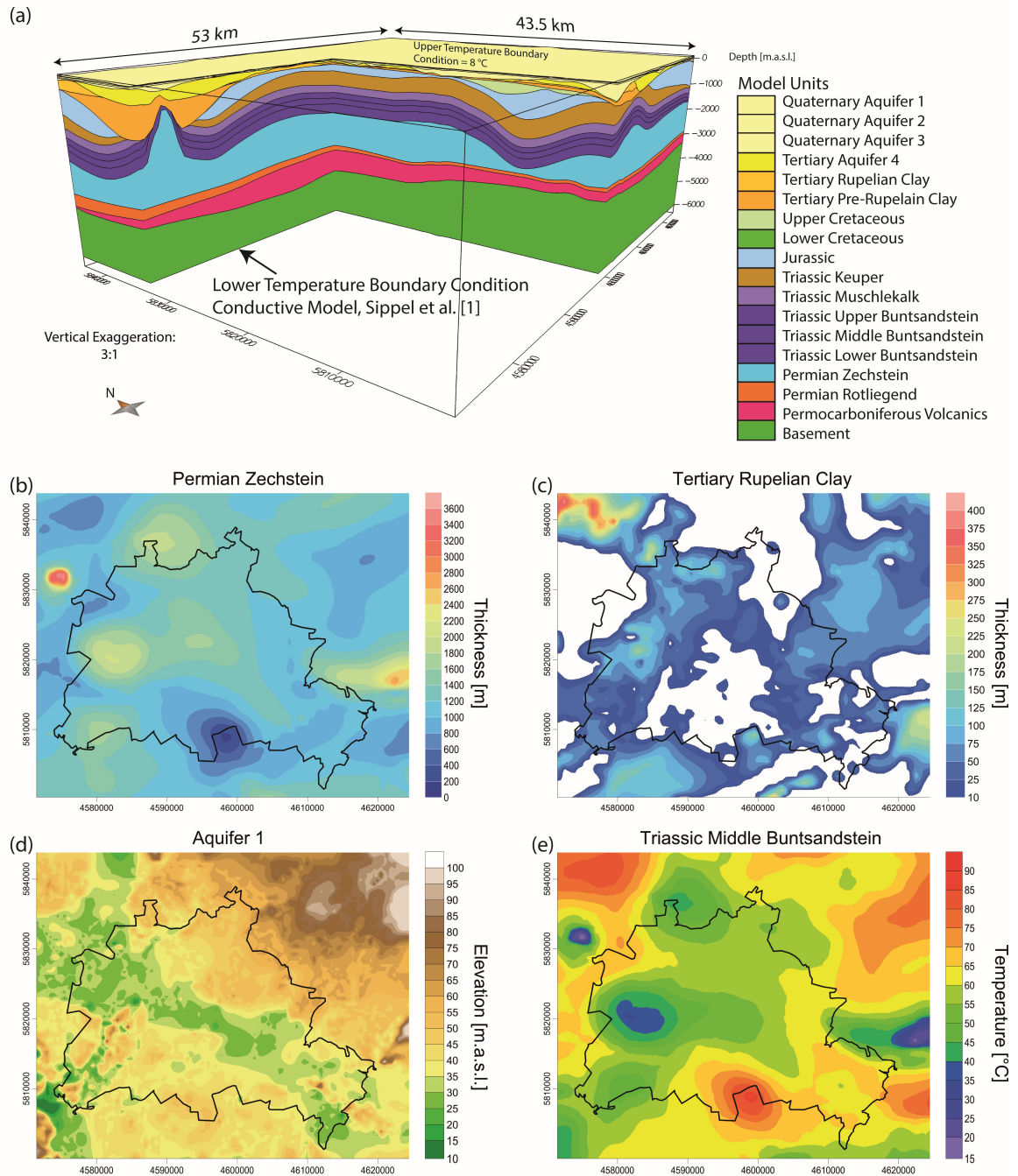


Figure 1: Reference model after Sippel et al. [1] used for the sensitivity analysis; black line in map shows political border of Berlin; coordinates [m] in Gauß-Krüger DHDN Zone 4 (a) Units of the 3D structural Model (b) Thickness distribution of Permian Zechstein (c) Thickness distribution of the Tertiary Rupelian Clay unit; white color indicates areas where the unit is absent (hydrogeological windows). (d) Elevation distribution of top of Aquifer 1 (top Model); m.a.s.l. meters above sea level. (e) Temperature distribution of the Reference Model at the top of the Triassic Middle Buntsandstein as predicted by coupled fluid-and-heat transport simulations.

### 3. Modeling Method

In order to carry out coupled heat and fluid simulations, the 3D geological model of the sedimentary basins as described in the previous section has been imported into the commercial software FEFLOW® [8]. The latter provides a finite element based computational framework to solve for (un)saturated groundwater flow in porous media taking into account conductive, advective and buoyant (fluid density related) heat transport processes. The mathematical formulation is based on a system of three coupled equation expressing conservation of fluid mass, momentum and energy as:

$$\frac{\partial[\epsilon\rho^{(l)}+(1-\epsilon)\rho^{(s)}]}{\partial t} + \nabla * (\epsilon\rho^{(l)}\mathbf{q}) = \epsilon Q^{(l)} + (1 - \epsilon)Q^{(s)} \quad (1)$$

$$\frac{\partial[\epsilon\rho^{(l)}c^{(l)}+(1-\epsilon)\rho^{(s)}c^{(s)}]T}{\partial t} = -\nabla * (\epsilon\rho^{(l)}c^{(l)}\mathbf{q} * T) - \nabla * [[(\lambda^{(b)}\mathbf{I}) + (\rho^{(l)}c^{(l)})\mathbf{D}] * \nabla T] + (1 - \epsilon)S \quad (2)$$

$$\mathbf{q} = -\frac{k}{\epsilon\mu}(\nabla p - \rho^{(l)}\mathbf{g}) \quad (3)$$

Table 1: Nomenclature of all parameters used in the numerical simulations

Parameter	Unit	Parameter	Unit
$c^0$	solid or fluid heat capacity	$q$	Darcy velocity
$D$	thermodispersivity tensor	$\epsilon$	porosity, void space fraction
$g$	gravity force	$\lambda^0$	fluid, solid of bulk thermal conductivity
$I$	unit tensor	$\rho^0$	fluid or solid density
$k$	permeability tensor of the porous medium	$\mu$	fluid dynamic viscosity
$p$	pressure	$\nabla$	Nabla operator
$S$	rock radiogenic heat production	$b$	bulk (liquid + solid)
$t$	time	$l$	liquid phase
$T$	temperature	$s$	solid phase
$Q^0$	fluid and solid mass source-sink term		

with (1) mass balance; (2) inertial energy balance for the system; (3) linear (Darcy's law) momentum conservation equation. An integration of an equation of state for the fluid density closes the partial differential equation problem. Accordingly, the fundamental relationships between the fluid state variables and the fluid density are represented. More details about the mathematical background and its numerical formulation can be found in Diersch et al. [8]. The horizontal resolution of the model is 200x200 m. To guarantee a good vertical-to-horizontal element shape ratio the original 18 geological units (Fig. 1a) with distinct geophysical properties were further subdivided, so that the final structural model is composed of 55 computational layers. As a result, every geological unit is composed of at least two computational layers displaying the same properties as the respective geological unit. All relevant physical rock and fluid properties adopted for all simulations are listed in Table 2.

All models have been run in transient state for both, fluid and heat flow, until reaching quasi-steady-state conditions. This state is assumed to be reached after a maximum of  $10^8$  d final simulation time with an initial time step length of  $10^{-3}$  d and a maximum time step length of  $5 \times 10^4$  d.

### 4. Model Scenarios and Modeling Results

In what follows, results from four simulations scenarios are described. Each model differs in terms of the surface boundary conditions (either thermal or hydraulic) imposed, while all other parameters and numerical settings are kept fixed. For all models, a variable thermal boundary condition has been imposed along the base of the model as obtained from the results of a lithosphere-scale conductive simulation [1]. This was done in order to integrate the amount of heat input in the total energy budget from the deeper crustal and mantle domains in the current simulations. All lateral boundaries are kept closed both to fluid and heat flow.



Table 2: Properties of the geological units as used for the thermal calculations.

Geological unit	Bulk thermal conductivity $\lambda^{(b)}$ [Wm-1K-1]	Radiogenic heat production S [μWm-3]	Rock heat capacity $c^{(s)}$ [kJkg-1K-1]	Effective porosity $\epsilon$ [-]	Permeability k [mD]
Aquifer1	3.5 <sup>f</sup>	0.9 <sup>c</sup>	2.16 <sup>d</sup>	0.311 <sup>d</sup>	10
Aquifer2	3.5 <sup>f</sup>	0.9 <sup>c</sup>	2.16 <sup>d</sup>	0.311 <sup>d</sup>	10
Aquifer3	3.5 <sup>f</sup>	0.9 <sup>c</sup>	2.16 <sup>d</sup>	0.311 <sup>d</sup>	10
Aquifer4	3.5 <sup>f</sup>	1.0 <sup>c</sup>	2.16 <sup>d</sup>	0.311 <sup>d</sup>	10
Rupelian clay	1.88 <sup>f</sup>	1.3 <sup>c</sup>	2.36 <sup>d</sup>	0.194 <sup>d</sup>	0.1
Pre-Rupelian clay	3.1 <sup>f</sup>	1.3 <sup>c</sup>	2.26 <sup>d</sup>	0.255 <sup>d</sup>	10
Upper Cretaceous	2.82 <sup>f</sup>	0.6 <sup>c</sup>	2.29 <sup>d</sup>	0.110 <sup>d</sup>	50
Lower Cretaceous	2.36 <sup>f</sup>	1.5 <sup>c</sup>	2.29 <sup>d</sup>	0.110 <sup>d</sup>	50
Jurassic	2.71 <sup>b</sup>	1.5 <sup>c</sup>	2.25 <sup>d</sup>	0.189 <sup>d</sup>	50
Keuper	2.35 <sup>b</sup>	1.6 <sup>c</sup>	2.32 <sup>d</sup>	0.128 <sup>d</sup>	10
Upper Muschelkalk	2.3 <sup>f</sup>	1.0 <sup>c</sup>	2.25 <sup>d</sup>	0.12 <sup>e</sup>	0.06 <sup>e</sup>
Middle Muschelkalk	2.3 <sup>f</sup>	1.0 <sup>c</sup>	2.25 <sup>d</sup>	0.036 <sup>e</sup>	1e-16 <sup>e</sup>
Lower Muschelkalk	2.3 <sup>f</sup>	1.0 <sup>c</sup>	2.25 <sup>d</sup>	0.15 <sup>e</sup>	1 <sup>e</sup>
Upper Buntsandstein	3.0 <sup>f</sup>	1.8 <sup>c</sup>	2.19 <sup>d</sup>	0.025	0.67
Middle Buntsandstein	2.0 <sup>f</sup>	1.8 <sup>c</sup>	2.39 <sup>d</sup>	0.135	60.76
Lower Buntsandstein	1.84 <sup>f</sup>	1.8 <sup>c</sup>	2.39 <sup>d</sup>	0.049	0.13
Zechstein	4.5 <sup>a</sup>	0.4 <sup>c</sup>	1.94 <sup>d</sup>	0.005	0.0001
Sedimentary Rotliegend	3.0 <sup>f</sup>	1.4 <sup>c</sup>	2.18 <sup>d</sup>	0.078	5.26
Permo-Carboniferous	2.5 <sup>c</sup>	2.9 <sup>d</sup>	2.60 <sup>d</sup>	0.032	0.09
Basement	2.2 <sup>d</sup>	2.8 <sup>d</sup>	2.30 <sup>d</sup>	0.01	1e-16

Parameter values were derived from (a) Norden et al. [9], (b) Fuchs and Förster [10], (c) Norden and Förster [11], (d) Norden et al. [12], (e) Pöppelreiter et al. [13] and (f) available temperature logs. Porosity values for the Upper Buntsandstein and underlying layers as well as all permeability values correspond to laboratory measurements of drill core material from the available four boreholes.

For the sake of readability, we present each model separately and postpone a discussion on their comparison for the next paragraph. The set of surface boundary conditions adopted for the first model presented, hereafter referred to as Reference Model, are a fixed temperature ( $T=8\text{ }^{\circ}\text{C}$ , as equals to averaged thermal surface conditions in northern Germany [14]) and a variable hydraulic head, which follows the surface topography.

The modeled thermal field is strongly imprinted by the lower thermal boundary condition imposed and the geological structuration of the different sedimentary units. This is more obvious at greater depths (larger than -2000 m.a.s.l.), where the thermal distribution shows a strong correlation with the surface topology and thickness of the highly conductive Zechstein Salt (Fig. 2d, [1]). Reaching shallower depth levels, the modeled thermal field displays a more complex configuration characterized by lateral variations of shorter wavelength than the deeper geothermal field. As a result, temperatures at -1000 m.a.s.l. range from 18.3 °C to 45.3 °C with several positive and negative anomalies distributed over the modeling area [1]. These variations can be explained by the highly heterogeneous distribution of topographic gradients (Fig. 1d). Areas of high topographic gradients are generally characterized by colder temperatures as induced by groundwater infiltrating from the top surface deeper in the model domain than in adjacent areas where such gradients are smoother. The complexity of this distribution decreases reaching larger depths (i.e. Fig. 1e) where a more homogenous distribution of the thermal field is evident (e.g. the temperature variations at -5000 m.a.s.l. are within a range of 146.0 °C to 174.2 °C). Here the temperature distribution follows the lower temperature boundary condition closely showing a decreasing trend from SE to NW.

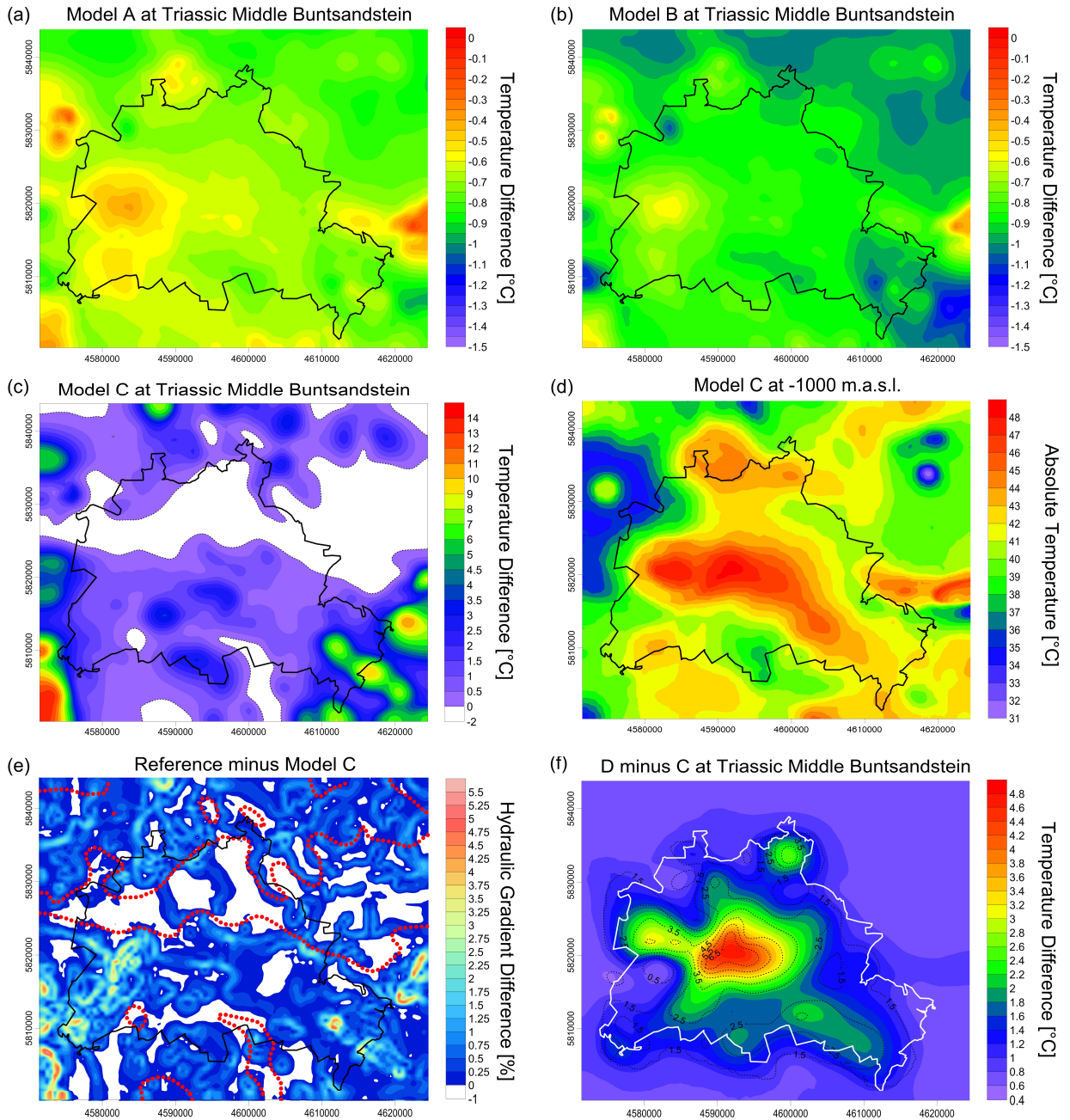


Figure 2: Results (coordinates [m] in Gauß-Krüger DHDN Zone 4). (a-c) Temperature differences between Models A, B, and C with respect to the reference model at top of Triassic Middle Buntsandstein. White color in (c) represents areas of temperatures that are lower than the ones predicted by the reference model. (d) Calculated temperatures at -1000 m.a.s.l. as predicted by Model C; m.a.s.l. meters above sea level. (e) Hydraulic gradient differences between the upper hydraulic head boundary condition of the reference model and of Model C; white color represents areas where the slope of Model C is higher than in the reference model and stippled red line refers to the transition from higher and lower temperatures predicted by Model C for the top of Triassic Middle Buntsandstein. (f) Temperature differences between Model D and Model C at the top of the Triassic Middle Buntsandstein; contour lines refer to the surface temperature differences between the models.

The boundary setting imposed for the reference model can be considered as a standard modelling option for large-scale groundwater and heat simulations of sedimentary basins (i.e. [15, 16]). However, it comes with some limitations due to oversimplification in the shallow surface thermal distribution and, especially, flow dynamics. While the groundwater table might resemble the regional scale topology of the surface topography in non-mountainous terrains as in Berlin, magnitudes of hydraulic head gradients do not always match gradients in topographic elevations. Therefore, the above described flow boundary conditions likely results in solving for an overpressured shallow system, thus accentuating the impact of advective heat transport by inflowing/outflowing groundwater from recharge/discharge areas.

In order to quantify the effects of these assumptions on the resulting thermal configuration, in a first series of simulations we have gradually lowered by a constant value the magnitude of imposed hydraulic head gradients from those considered in the reference model while maintaining the regional morphology of the groundwater table as in the previous study case. We present the results from two model realizations in which the groundwater head has been lowered by a fixed amount equal to 10 m (Model A) and 20 m (Model B).

Sensitivities for all models have been tested with the parameters and properties described in section 3 and 4. Accordingly assessments of the sensitivity of the models of this study to changes in temperature and pressure are expressed in differences of calculated temperatures to the reference model. An exception had to be done for the last approach where results are shown in comparison to Model C (see last paragraph of this section).

Modeling results for scenarios A and B predict temperatures that are generally colder than those predicted by the reference model (Fig. 1e, 2a, b). At -1000 m.a.s.l. temperature differences range between  $+0.05^{\circ}\text{C}$  and  $-1.15^{\circ}\text{C}$  (Model A), and  $-0.15^{\circ}\text{C}$  and  $-1.3^{\circ}\text{C}$  (Model B). These ranges decrease at higher depths (-5000 m.a.s.l.) to mean values of  $-0.5^{\circ}\text{C}$  (Model A) and  $-0.55^{\circ}\text{C}$  (Model B) with a deviation of  $\pm 0.13^{\circ}\text{C}$ . Temperature differences at the top of the Middle Buntsandstein are on average  $-0.7^{\circ}\text{C}$  for Model A (Fig. 2a) and  $-0.88^{\circ}\text{C}$  for Model B (Fig. 2b). Since temperature differences are small, predicted absolute temperatures show similar patterns to those of the reference model (Fig. 1e). However, absolute temperature differences are distributed heterogeneously across the model area with lowest differences located in the E, W and SW.

Models A and B should be considered as a simplistic attempts towards a sensitivity study, in that the top hydraulic boundary conditions have been fixed ad hoc on the model. In a second stage, we opted for a more detailed investigation on the sensitivity of model outcomes to variations on the surface boundary conditions. At this purpose, hydraulic head data as available for the city of Berlin [17] have been integrated as fixed, 1<sup>st</sup> type, boundary (Model C, Fig. 3a).

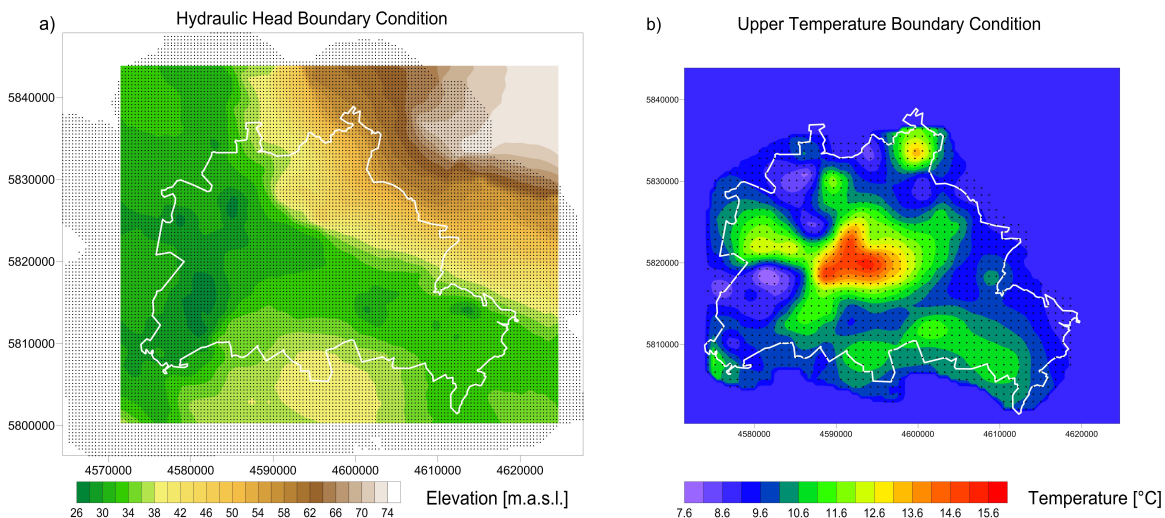


Figure 3: Upper boundary conditions (m.a.s.l. meters above sea level; coordinates [m] in Gauß-Krüger DHDN Zone 4). (a) Hydraulic head (data from Senate Department for Urban Development and the Environment, [17]); data coverage indicated by black dots, while colored area represents model extent. (b) Temperatures at groundwater table (data from Senate Department for Urban Development and the Environment, [18]) data coverage indicated by black dots, colored area represents model extent.

The hydraulic head distribution approximately follows the topography but does not display lateral short wavelength elevation changes. Highest values are found in the NE and S while lowest values are to the E and SE. Groundwater flow therefore trends towards the E and SE displaying a gentle hydraulic gradient over the whole model area.

Results for this approach show a rather different trend in modeling results compared to Models A and B (Fig. 2c). The differences in temperatures to the reference model are up to an order of magnitude higher and reach maximum values of +18.6 °C. At -1000 m.a.s.l. Model C predicts on average +1.36 °C (at -5000 m.a.s.l. it lowers to a value of +0.11 °C). Within the target horizon (Triassic Middle Buntsandstein) calculated temperatures differ on average by +1.24 °C from the reference model with a maximum of +13.78 °C (Fig. 2c). In contrast to the results from the first approach the distribution of these differences is highly heterogeneous. While the central part of the model area displays little to no change, the outer model domains display areas of high temperature difference in the SE, SW and NW.

In a last attempt we implemented measured temperature data [18] additionally to the measured hydraulic head data (Model D). These data cover only parts of the model (running approximately along the city borders). For areas outside the data coverage, a constant value of 9 °C had been assigned as being representative for uncultivated and less populated areas [14, 19], Fig. 3b. Higher temperatures in the center of Berlin correlate with highest surface sealing and or population density.

Since the available data covers the temperature distribution at the groundwater level, we limit our discussion to a comparison between the obtained results with those described from Model C. Assigned temperature differences at the top of the model are as high as +7.3 °C with an average of +1.64 °C (Fig. 2f). Quantitatively, the differences between models C and D are up to +5.12 °C (-1000 m.a.s.l.) at investigated depth levels with highest differences predicted at shallow levels and lowest differences at deeper levels of the model. Predicted temperatures at -5000 m.a.s.l. are only up to 1.0 °C higher than those calculated by Model C. Differences at the target horizon Middle Buntsandstein have a mean value of +1.21 °C with a maximum of +4.75 °C. The distribution of those differences shows that highest differences are at the center of the modeling area displaying a decreasing trend towards the model boundaries.

## 5. Discussion & Conclusion

In the course of this work, a regional 3D geothermal model of coupled fluid flow and heat transport of the Berlin area has been tested concerning sensitivities of computed temperatures to upper boundary conditions (HHBC; TBC) where previous studies failed to fully reconcile observations by underestimating the thermal conditions in the shallow subsurface [1, 20]. The observed misfit between model and measurements has been related to two major assumptions integrated in those numerical investigations, that is: (1) an oversimplification of the upper HHBC and (2) simplified geological characterization of the shallow Late Tertiary and Quaternary aquifer/aquitard system. This study focuses on a quantification of the influences of the upper BC on model temperatures thus targeting the first aspect as described above.

In a first attempt, variations of surficial hydraulic head gradients have been systematically imposed along the top surface of the model by gradually lowering its reference value (set equals to the topographic elevations). Predicted subsurface temperatures only change little and are on average colder (max.: -1.0 °C; -1.3 °C). Interestingly, the amount of cooling correlates with the Zechstein thickness distribution (Fig. 1c, 2a, b). We therefore hypothesize, that in areas where the Zechstein is thick (Fig. 1c), conductive heat transport processes are able to compensate the influence of advection by groundwater pressure gradients (areas of negligible temperature difference). Thereby, in areas with a large thickness of the thermally conductive Zechstein salt, the influence of the groundwater component of heat transport is largely compensated so that the modelled temperatures do hardly differ from a purely conductive case [1]. Additionally the small magnitude and range of changes in predicted temperatures suggest that the overall elevation of the upper HHBC plays a minor role in geothermal modeling when the latter is simplified to account for the regional topographical elevation.

In contrast, implementing measured hydraulic head data as upper HHBC leads to significant changes in the predicted subsurface temperature field. The lateral range of temperatures for the investigated depth levels decreases considerably (27 °C to 16 °C at -1000 m.a.s.l.) whilst temperatures are also up to 19 °C higher compared to the reference model. In areas where the gradient of the HHBC was reduced compared to the reference model, higher temperatures are predicted and vice versa (Fig. 2c, e). From looking at a map of constant depth (Fig. 2d) it becomes



evident, that this approach predicts temperatures which follow unit geometries (Fig. 1c) more closely than for models where the actual geometry of the groundwater table is not considered.

Conclusively, these results show that the local geometry of the upper HHBC has a strong influence on modelled temperatures across the whole model domain. The overall correlation between imposed changes in hydraulic gradient and predicted temperatures is lacking for a closed domain located in the SW corner of the study area where, despite hydraulic gradients having been drastically reduced, only relative small temperature changes have been observed. However, this area is underlain by a relative thick sequence of highly conductive, but impervious to groundwater flow, Zechstein salt (thickness up to 2000 m, Fig. 1c). Based on these observations we can conclude that for this specific domain, heat is principally transported by conduction while additional processes related to groundwater flow are only of minor importance.

When additional measurements of the groundwater temperature distribution are considered, computed temperatures show some difference with those obtained from model realization adopting a constant fixed value. By changing the surface temperature by up to 7.3 °C, we calculate higher subsurface temperatures than for a constant model. Not surprisingly, magnitudes of these deviations decrease linearly with depth where the influence of the lower boundary conditions starts to dominate the thermal configuration (max.: 1.0 °C at -5000 m.a.s.l.). Temperature differences across the model area are distributed in a comparatively simple manner. Where changes in the applied upper TBC are highest at the top, changes in the subsurface are also at their maximum (Fig. 2f). Since higher measured temperatures are likely linked to surface sealing and urbanization [14, 19], the anthropogenic influence on the subsurface thermal field becomes evident.

The results from the different modelling realizations have also been discussed in terms of temperature distribution within the Middle Buntsandstein unit, the latter being a preferential target horizon for geothermal exploration in the study area. This was done in order to ease the discussion toward implications for a practical utilization of geothermal energy. The model results show that, depending on the degree of approximation adopted to represent surface hydraulic conditions, different temperature distributions can be predicted within the targeted horizon. Higher temperatures (up to 15 °C) within the Buntsandstein have been predicted for those models, which integrate observed variations in the groundwater table when compared to realizations where the top hydraulic boundary conditions was approximated as a subdued replica of the topographic relief. Observed variations in the temperature distribution at depths greater than 2 km clearly indicate the importance of an adequate and detailed implementation of the shallow groundwater dynamics for regional basin studies for geothermal exploration.

This study is part of an ongoing investigation aiming at meliorating the current understanding of the thermal and hydraulic configuration within the area of Berlin. In doing so, we rely on numerical modelling techniques which enable to integrate available hydrogeological information into a robust mathematical framework thus permitting the quantification of each relevant process affecting the present thermal and hydraulic setting in the study area. More precisely, the principal aim of this study was to investigate the impact of commonly followed assumptions regarding the surface conditions on the regional hydro-thermal configuration of the system at depth. The study has provided a deeper and quantitative understanding of the thermal signature of processes occurring at the surface and their interaction with the spatial distribution of rock properties as imposed by the actual geology of the system. The results suggest a close correlation between the assumed surface hydrodynamics and the complex geology underneath Berlin, which likely lead to different thermal conditions even at depth levels of interest for potential geothermal energy utilization. Efforts are currently made to improve the resolution of the shallow groundwater compartments by integrating newly available geological information on the late Tertiary-Quaternary sedimentary units in order to resolve details of the subsurface interactions between geology, shallow and deeper groundwater circulation on the resulting thermal configuration that were not yet addressed by previous investigation in the study area.

## Acknowledgements

We would like to thank the Senate Department for Urban Development and the Environment for providing the data for this study.

## References

- [1] Sippel J, Fuchs S, Cacace M, Kastner O, Huenges E, Scheck-Wenderoth M. Deep 3D thermal modelling for the city of Berlin (Germany). *Environ Earth Sci* 2013.
- [2] Maystrenko Y, Bayer U, Scheck-Wenderoth M, Structure and Evolution of the Central European Basin System according to 3D modeling, in: DGMK Research Report 577, 2010.
- [3] Maystrenko Y, Bayer U, Scheck-Wenderoth M. Salt as a 3D element in structural modeling - Example from the Central European Basin System. *Tectonophysics in press, accepted June 2012* 2012.
- [4] Scheck M, Bayer U. Evolution of the Northeast German Basin - inferences from a 3D structural model and subsidence analysis. *Tectonophysics* 1999; 313: 145-169.
- [5] Scheck M, Bayer U, Lewerenz B. Salt movement in the Northeast German Basin and its relation to major post-Permian tectonic phases - results from 3D structural modelling, backstripping and reflection seismic data *Tectonophysics* 2003; 361: 277-299.
- [6] Huenges E, Ledru P. *Geothermal energy systems: exploration, development, and utilization*. John Wiley & Sons; 2011.
- [7] Limberg A, Thierbach J. Hydrostratigraphie von Berlin-Korrelation mit dem Norddeutschen Gliederungsschema. *Brandenburgische Geowiss. Beitr* 2002; 9: 2.
- [8] Diersch H-J. *FEFLOW Finite Element Subsurface Flow & Transport Simulation System, Reference Manual*. Berlin: WASY GmbH Institute for Water Resources Planning and System Research; 2009.
- [9] Norden B, Förster A, Balling N. Heat flow and lithospheric thermal regime in the Northeast German Basin *Tectonophysics* 2008; 460: 215-229.
- [10] Fuchs S, Förster A. Rock thermal conductivity of Mesozoic geothermal aquifers in the Northeast German Basin. *Chem Erde Geochem* 2010; 70: 13-22.
- [11] Norden B, Förster A. Thermal conductivity and radiogenic heat production of sedimentary and magmatic rocks in the Northeast German Basin. *AAPG Bull* 2006; 90: 939-962.
- [12] Norden B, Förster A, Behrends K, Krause K, Stecken L, Meyer R. Geological 3-D model of the larger Altensalzwedel area, Germany, for temperature prognosis and reservoir simulation. *Environ Earth Sci* 2012; 67: 511-256.
- [13] Pöppelreiter M, Borkhataria R, Aigner T, Pipping K. Production from Muschelkalk carbonates (Triassic, NE Netherlands): unique play or overlooked opportunity? *Geological Society, London, Petroleum Geology Conference series* 2005; 6: 299-315.
- [14] Henning A, Limberg A. Veränderung des oberflächennahen Temperaturfeldes von Berlin durch Klimawandel und Urbanisierung. *Brandenburgische Geowiss. Beitr* 2012; 19 (2012): 81-92.
- [15] Garven G, Freeze RA. Theoretical analysis of the role of groundwater flow in the genesis of stratabound ore deposits; 1, Mathematical and numerical model. *Am J Sci* 1984; 284: 1085-1124.
- [16] Person M, Garven G. A sensitivity study of the driving forces on fluid flow during continental-rift basin evolution. *Geol Soc Am Bull* 1994; 106: 461-475.
- [17] SenStadtUm, 02.12 Grundwasserhöhen des Hauptgrundwasserleiters und des Panketalgrundwasserleiters (Ausgabe 2013), in: Grundwassermanagement Gu (Ed.), Senatsverwaltung für Stadtentwicklung und Umwelt, Berlin, 2013.
- [18] SenStadtUm, 02.14 Grundwassertemperatur (Ausgabe 2014), in: Grundwassermanagement Gu (Ed.), Senatsverwaltung für Stadtentwicklung und Umwelt, Berlin, 2014.
- [19] Menberg K, Bayer P, Zosseder K, Rumohr S, Blum P. Subsurface urban heat islands in German cities. *Sci Total Environ* 2013; 442: 123-133.
- [20] Noack V, Scheck-Wenderoth M, Cacace M, Schneider M. Influence of fluid flow on the regional thermal field: results from 3D numerical modelling for the area of Brandenburg (North German Basin). *Environ Earth Sci* 2013.